Combined X-ray Diffraction and ^{15}N CPMAS NMR Study of Molecular Structure and Proton Order/Disorder Phenomena in Cyclic *N*,*N*′-Bisarylformamidine Dimers

Romana Anulewicz,[†] Iwona Wawer,[‡] Tadeusz Marek Krygowski,*[,†] Ferdinand Männle,[§] and Hans-Heinrich Limbach*[,§]

Contribution from the Department of Chemistry, Warsaw University, ul.Pasteura 1, Pl-02093 Warsaw, Poland, Faculty of Pharmacy, Medical Academy, Pl-02097 Warsaw, Poland, and Institut für Organische Chemie, Freie Universität Berlin, Takustrasse 3, D-14195 Berlin, Germany

Received March 4, 1997. Revised Manuscript Received July 17, 1997[⊗]

Abstract: Crystal structures of a series of five symmetrically substituted *N*,*N*-bisarylformamidines ArNH−CH═NAr with Ar = X-C_6H_4, X = *p*-OCH_3 (**IV**), *p*-CH_3 (**V**), *p*-F (**VI**), *p*-NO_2 (**VII**), and *m*-Br (**VIII**) have been determined by single-crystal X-ray diffraction (XRD) and complete the series studied previously where X = H (**I**), *p*-Br (**II**), and *p*-Cl (**III**). In addition, the results of variable-temperature ^{15}N CPMAS NMR experiments performed on ^{15}N-labeled **I**, **II**, and **IV** are reported. All compounds form cyclic dimers linked by two N−H···N hydrogen bonds which can form two different tautomers, a and b, interconverting by fast double proton transfers. The NMR experiments indicate three types of amidines characterized by different magnitudes of the equilibrium constants K_{ab} of the tautomerism. In dimers of type such as **V**−**VIII,** we find $K_{ab} \ll 1$ (i.e., only a single tautomer in the temperature range between 100 and 300 K). In this case, the hydrogen-bonded protons are ordered and can be localized by XRD. Furthermore, the C···N bond lengths and torsional and valence angles involving the two aryl groups of an amidine unit are different. For dimers such as **II** and **III,** characteristic temperature dependent ^{15}N CPMAS NMR line shape changes are observed indicating that $K_{ab} = 1$ within the margin of error. Rate constants of the tautomerism can in this case be obtained by line shape analysis. For this degeneracy to occur, the aryl group conformations at both amidine nitrogen atoms must be similar. XRD then observes disordered hydrogen-bond protons and, in principle, also disordered nitrogen atoms. However, in practice, the disorder of the latter is not resolved leading to the observation of equalized C···N bond lengths. Finally, dimers (**I**, **IV**) represent an intermediate case with $K_{ab} < 1$, which could be labeled as "dynamic partial order". The implications of the molecular structure and the hydrogen bond and proton transfer characteristics are discussed.

Introduction

Substituted amidines are the nitrogen analogs of carboxylic acids and have been studied by various spectroscopic techniques.[1−4] As shown by NMR,[2,3] both *s-cis* and *s-trans* conformers (Figure 1a) can be present in solution exhibiting different hydrogen-bond association patterns. Evidence was obtained that only the *s-trans* conformers are able to form cyclic hydrogen-bonded dimers (Figure 1b) in which fast double proton transfers can take place,[3] in analogy to carboxylic acid dimers. On the other hand, X-ray diffraction techniques (XRD) showed that neither substituted acetamidines nor benzamidines form cyclic dimers in the solid state.[5,6] These species have, however, finally been observed in recent years in the case of some *N*,*N*-bisarylformamidines with the aryl substituents phenyl (**I**),[7] *p*-bromophenyl (**II**),[8] and *p*-chlorophenyl (**III**).[9] In these compounds the amidine planes are generally not planar; in addition,[7−9] the aryl rings are considerably twisted out from the amidine planes. The observed twist angles result from the balance between the potential coupling of these two π-electron systems and the steric and other components of the crystal packing forces.

By contrast, details of the hydrogen bonding of these compounds could not be studied because of the well-known problems of XRD[10] in characterizing the position and dynamics of hydrogen-bond protons. Usually, this method distinguishes between the situations of "proton order" and "static vs dynamic

[†] Warsaw University.
[‡] Medical Academy.
[§] Freie Universität Berlin.
[⊗] Abstract published in *Advance ACS Abstracts,* November 15, 1997.

(1) (a) Häfelinger, G. in *The Chemistry of Amidines and Imidates*; Patai, S., Ed.; Wiley: London, 1975; Vol. 1, Chapter 1, p 1.
(2) Borisov, D. N.; Kratsov, D. N.; Peregudov, A. S.; Fedin, E. I. *Izv. Akad. Nauk. SSSR, Ser. Khim.* **1980**, 2151.
(3) (a) Meschede, L.; Gerritzen, D.; Limbach, H.-H. *Ber. Bunsen-Ges. Phys. Chem.* **1988**, 92, 5669. (b) Limbach, H.-H.; Meschede, L.; Scherer, G. *Z. Naturforsch.* **1989**, *44a*, 459. (c) Meschede L.; Limbach, H.-H. *J. Phys. Chem.* **1991**, *95*, 10267 and references cited therein.
(4) (a) Raczynska, E. D.; Laurence Ch. *Analyst* **1992**, *117*, 375. (b) Anulewicz R.; Krygowski, T. M.; Raczynska, E. D. *J. Phys. Org. Chem.* **1991**, 331.
(5) Krygowski, T. M.; Wozniak, K. In *The Chemistry of Amidines and Imidates;* Patai, S., Rappoport, Z., Eds.; Wiley: New York, 1991; Vol. 2, Chapter 2, p 101.
(6) (a) Krajewski, J.; Urbanczyk-Lipkowska, Z.; Gluzinski, P.; Oszczapowicz, J.; Busko-Oszczapowicz, I.; Bleidelis, J.; Kemme, A. *Pol. J. Chem.* **1981**, *55*, 1015. (b) Norrestam, R.; Mertz, S.; Crossland, I. *Acta Crystallogr.* **1983**, *C39*, 1554. (c) Norrestam, R. *Acta Crystallogr.* **1948**, *C40*, 955. Gilli, G.; Bertolasi,V. *J. Am. Chem. Soc.* **1979**, *101*, 7704. (d) Kosturkiewicz, Z.; Ciszak, E.; Tykarska, E. *Acta Crystallogr.* **1992**, *B48* 471.
(7) Anulewicz, R.; Krygowski, T. M.; Pniewska, B., *J. Cryst. Spectrosc. Res.* **1987**, *17*, 661.
(8) Anulewicz, R.; Krygowski, T. M.; Jaroszewska-Manaj, J.; Pniewska, B. *Pol. J. Chem.* **1991**, *65*, 465.
(9) Anulewicz, R.; Krygowski, T. M.; Pniewska, B. *Acta Crystallogr.* **1990**, *C46*, 2121.
(10) Trueblood, K. N. In *Accurate Molecular Structures, Their Determination and Importance*; Domenicano, A., Hargittai, I., Eds.; Oxford University Press: 1992; Chapter 8, p 200.

S0002-7863(97)00699-9 CCC: $14.00

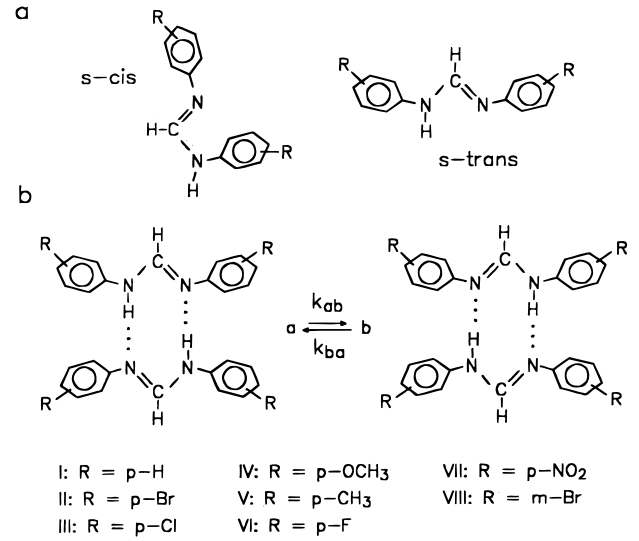

Figure 1. (a) The *s-cis* and *s-trans* conformers of *N*,*N*′-bisarylformamidines in solution according to refs 2 and 3. (b) Double proton transfer in cyclic *N*,*N*′-bisarylformamidines dimers: *N*,*N*′-bisphenylformamidine (**I,** type C), *N*,*N*′-bis(*p*-bromophenyl)formamidine (**II,** type B), *N*,*N*′-bis(*p*-chlorophenyl)formamidine (**III,** type B), *N*,*N*′-bis(*p*-methoxyphenyl)formamidine (**IV**, type C), *N*,*N*′-bis(*p*-methylphenyl)formamidine (**V,** type A), *N*,*N*′-bis(*p*-fluorophenyl)formamidine (**VI,** type A), *N*,*N*′-bis(*p*-nitrophenyl)formamidine (**VII** type A), *N*,*N*′-bis(*m*-bromophenyl)formamidine (**VIII,** type A).

proton disorder". These terms are, however, not easily related to the thermodynamics and kinetics of proton transfer accessible by solid state NMR.[11−15] For example, in the case of carboxylic acids, various single-crystal ^{1}H and ^{2}H NMR methods have been used to follow the proton transfer dynamics.[11] In the case of proton transfer from and to nitrogen, it has been shown that high-resolution solid state ^{15}N NMR of ^{15}N-enriched compounds under the conditions of cross polarization (CP), magic angle spinning (MAS), and proton decoupling is especially useful, since this method does not require single crystals. Using this method, a number of double, triple, and quadruple intermolecular proton transfers in solid pyrazoles have been detected[12] and also a number of intramolecular proton transfers.[13−15] In a recent ^{15}N CPMAS NMR study of ^{15}N-labeled **II**, it was shown that this compound not only forms cyclic hydrogen-bonded dimers in the solid state but that these dimers also exhibit fast double proton transfers as the carboxylic acids.[16]

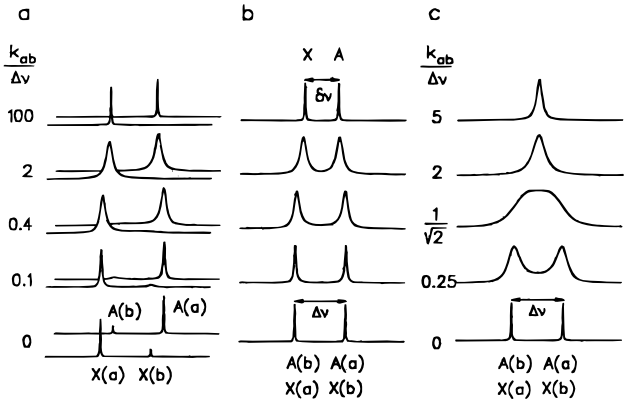

Figure 2. Calculated NMR spectra for two single spins A and X located in a molecule subject to exchange between two molecular states a and b according to eq 1. For further description see the text.

Since amidines form coupled N−H···N hydrogen bonds, they can be regarded as model systems for nucleic acids base pairing, and it may not be an hazard that the amidine skeleton R−NH−C(R)=N−R is often a part of important chemical compounds which serve as antivirial, antibacterial, antifungial, antihypertensive, and tranquilizing drugs; some amidines are active and/or have been tested as potential cancer chemotherapeutics.[17]

Thus, we felt motivated to now study a larger number of crystalline *N*,*N*-bisarylformamidines by combined XRD and ^{15}N NMR techniques in order to evaluate the influence of the chemical and crystal structure—especially of the aryl twist angles—on the hydrogen-bond properties of these compounds. Here, we report the result of XRD of five symmetric *N*,*N*-bisarylformamidines **IV**−**VIII** with varying substitutents and present some new ^{15}N CPMAS NMR results of selected amidines which had to be isotopically enriched for this purpose. Depending on the chemical and crystal structure, we find that the gas-phase degeneracy of the double proton transfer is more or less perturbed, which is not only manifest in the NMR spectra but also leads to characteristic structural changes.

This paper is organized as follows. After a short Theoretical Section in which dynamic high-resolution NMR is shortly reviewed with respect to the case of proton transfer in solid amidines as observed by ^{15}N NMR and with respect to the proton order/disorder problem encountered in XRD, followed

(11) (a) Meier, B. H.; Graf, F.; Ernst, R. R. *J. Chem. Phys*. **1982**, *76*, 768. (b) Meyer, R.; Ernst, R. R. *J. Chem. Phys*. **1990**, *93*, 768. (c) Heuer, A.; Haeberlen, U. *J. Chem. Phys*. **1991**, *95*, 4201. (d) Stöckli, A.; Maier, B. H.; Kreis, R.; Meyer, R.; Ernst, R. R. *J. Chem. Phys*. **1990**, *93*, 15002.

(12) (a) Smith, J. A. S.; Wehrle, F.; Aguilar-Parilla, F.; Limbach, H.-H.; Foces-Foces, M. C.; Cano, F. H.; Elguero, J.; Baldy, A.; Pierrot, M.; Khurshid M. M. T.; Lacombe-McDual, J. B. *J. Am. Chem. Soc*. **1989**, *111*, 7304. (b) Aguilar-Parilla, F.; Scherer, G.; Limbach, H.-H.; Foces-Foces, M. C.; Cano, F. H.; Smith, J. A. S.; Toiron, C. Elguero, J. J. *J. Am. Chem. Soc*. **1992**, *114*, 9657. (c) Aguilar-Parrilla, F.; Cativiela, C.; Diaz de Villegas, M. D.; Elguero, J.; Foces-Foces, C.; Laureiro, J. I. G.; Cano, F. H.; Limbach, H.-H.; Smith, J. A. S.; Toiron, C. *J. Chem. Soc., Perkin Trans. 2* **1992**, 1737. (d) Elguero, J.; Cano, F. H.; Foces-Foces, C.; Llamas-Saiz, A. L.; Limbach, H.-H.; Aguilar-Parrilla, F.; Claramunt, R. M.; Lopez, C. *J. Heterocycl. Chem.* **1994**, *31*, 695. (e) Aguilar-Parrilla, F.; Limbach, H.-H.; Foces-Foces, C.; Cano, F. H.; Jagerovic, N.; Elguero, J. *J. Org. Chem.* **1995**, *60*, 1965. (f) Elguero, J.; Jagerovic, N.; Foces-Foces, C.; Cano, F. H.; Roux, M. V.; Aguilar-Parrilla, F.; Limbach, H.-H. *J. Heterocycl. Chem.* **1995**, *32*, 451.

(13) (a) Limbach, H.-H.; Hennig, J.; Kendrick, R. D.; Yannoni, C. S. *J. Am. Chem. Soc.* **1984**, *106*, 4059. (b) Kendrick, R. D.; Friedrich, S.; Wehrle, B.; Limbach, H.-H.; Yannoni, C. S. *J. Magn. Reson*. **1985**, *30*, 159. (c) Wehrle, B.; Limbach, H.-H.; Köcher, M.; Ermer, O.; Vogel, E. *Angew. Chem.* **1987**, *99*, 914; *Angew. Chem. Int. Ed. Engl.* **1987**, *26*, 934. (d) Limbach, H.-H.; Wehrle, B.; Zimmermann, H.; Kendrick, R. D.; Yannoni, C. S. *J. Am. Chem. Soc*. **1987**, *109*, 929. (e) Limbach, H.-H.; Wehrle, B.; Zimmermann, H.; Kendrick, R. D.; Yannoni, C. S. *Angew. Chem.* **1987**, *99*, 241; *Angew. Chem., Int. Ed. Engl*. **1987**, *26*, 247. (f) Wehrle, B.; Limbach, H.-H.; Zimmermann, H. *Ber. Bunsen-Ges. Phys. Chem*. **1987**, *91*, 941. (g) Limbach, H.-H.; Wehrle, B.; Schlabach, M.; Kendrick, R. D.; Yannoni, C. S. *J. Magn. Reson.* **1988**, *77*, 84. (h) Wehrle, B.; Zimmermann, H.; Limbach, H.-H. *J. Am. Chem. Soc.* **1988**, *110*, 7014. (i) Wehrle, B.; Limbach, H.-H. *Chem. Phys.*, **1989**, *136*, 223. (j) Schlabach, M.; Wehrle, B.; Braun, J.; Scherer, G.; Limbach, H.-H. *Ber. Bunsen-Ges. Phys. Chem.* **1992**, *96*, 821. (k) Braun, J.; Schlabach, M.; Wehrle, B.; Köcher, M.; Vogel, E.; Limbach, H.-H. *J. Am. Chem. Soc.* **1994**, *116*, 6593. (l) Hoelger, C. G.; Wehrle, B.; Benedict, H.; Limbach, H.-H. *J. Phys. Chem.* **1994**, *98*, 843.

(14) Limbach, H.-H. In *NMR Basic Principles and Progress, Vol. 23*: *Deuterium and Shift Calculation*; Springer-Verlag Heidelberg, 1991; Chapter 2, pp 66−167.

(15) Limbach, H.-H.; Scherer G.; Meschede, L.; Aguilar-Parrilla, F.; Wehrle, B.; Braun, J.; Hoelger, Ch.; Benedict, H.; Buntkowsky, G.; Fehlhammer, W. P.; Elguero, J.; Smith, J. A. S.; Chaudret, B. NMR studies of Elementary Steps of Hydrogen Transfer in Condensed Phases. *In Ultrafast Reaction, Dynamics and Solvent Effects, Experimental Aspects*; Gaudel, Y., Rossky, P. J., Eds.; American Institute of Physics: Woodbury, NY, 1993.

(16) Männle F.; Wawer I.; Limbach H. H. *Chem. Phys. Lett.* **1996**, *256*, 667.

(17) Grout, R. J. In *The Chemistry of Amidines and Imidates*; Patai, S., Ed.; Wiley: New York, Chichester, 1975; Chapter 6 and references cited therein.

Table 1. Selected Bond Lengths, Valence Angles, and Torsion Angles of Cyclic Bisarylformamidine Dimers

R	type of dimer	C1···N1	C1···N2	N1···N2′	H1···H9[b]	H1···H3[b]	α_1	α_2	$\Delta = \alpha_1 - \alpha_2$	ϕ_1	ϕ_2	N1−C1−N2
I[a] (*p*-H)[7]	C	1.311	1.323	3.010	2.069	2.210	120.1	120.3	0.2	59.3	9.3	122.1
		1.305	1.314	2.984	2.241	2.116	119.8	120.5	0.7	37.7	30.7	123.0
II[a] (*p*-Br)[8]	B	1.311	1.311	2.963			123.3	123.3	0	24.4	24.4	121.0
		1.313	1.313	2.963			121.3	121.3	0	30.3	30.3	122.8
III[a] (*p*-Cl)[9]	B	1.312	1.312	2.958			122.9	122.9	0	27.0	27.0	121.0
		1.309	1.309	2.958			121.6	121.6	0	42.7	42.7	122.8
IV[a] (*p*-OCH_3)	C	1.308	1.315	2.973	2.336	2.243	118.5	120.2	1.7	41.9	36.3	124.7
		1.306	1.311	3.038	2.211	2.295	123.3	123.5	0.2	23.5	28.0	122.1
V (*p*-CH_3)	A	1.280	1.346	3.063	2.372	2.214	116.5	124.0	7.5	44.4	27.1	123.3
VI[a] (*p*-F)	A	1.281	1.349	2.975	2.432	2.165	115.9	126.1	10.2	44.3	12.1	122.2
		1.283	1.342	3.093	2.686	2.114	118.2	126.3	8.1	58.7	1.3	122.6
VII (*p*-NO_2)	A	1.282	1.360	3.063	2.330	2.083	115.6	123.7	8.5	45.4	9.4	122.0
VIII (*m*-Br)	A	1.296	1.356	3.049	2.549	1.951	114.7	124.7	10.0	47.3	7.9	122.4

[a] Two independent molecules in a dimer. All distances are in angstroms, and all angles are in degrees. For atom numbering, see Figure 3. The classification into different types were done by NMR for **I**, **II**, and **V** and by XRD for the others. [b] Sum of van der Waals radii 2.4 Å according to ref 27.

by short Experimental Section, the Results will be presented and discussed.

Theoretical Section

In this section, we consider the effects of an interconversion between two tautomeric states, a and b, adopted by each hydrogen-bond unit in a crystal on the NMR spectra of the two heavy nuclei A and X, here assumed to be ^{15}N atoms. This equilibrium can be written as

$$\mathrm{a} \equiv \mathrm{A{-}H{\cdots}X} \underset{k_{ba}}{\overset{k_{ab}}{\rightleftharpoons}} \mathrm{b} \equiv \mathrm{A{\cdots}H{-}X} \qquad (1)$$

Since this problem has been described previously,[13−15] we present only a brief review of the expected line shape patterns. In addition, we discuss the crystallographic terms "proton order" and "static/dynamic proton disorder" as special cases of eq 1, as described previously.[12]

As a convention, we assign here tautomer a to the dominantly populated state. The equilibrium constant characterizing eq 1 is defined by

$$K_{ab} = x_b/x_a = k_{ab}/k_{ba} \qquad (2)$$

and is the same for each proton transfer unit; k_{ij} is the rate constant of the reaction from state i to j and x_i the mole fraction of state i. The exchange of eq 1 leads to a modulation of the chemical shift of the nuclei A between $\nu_A(a)$, characterized by the mole fraction x_a, and ν_A-(b), characterized by x_b. In a similar way, nucleus X exchanges between the positions $\nu_X(a)$ and $\nu_X(b)$. This model leads in the slow-exchange regime to a spectrum shown at the bottom of Figure 2a, where the line shape contributions of A and X have been separated for clarity. As k_{ab} is increased, line A(a) shows first an exchange broadening of k_{ab}/π and A(b) of k_{ba}/π, and the coalescence to a single line with the averaged position

$$\nu_A = x_a\nu_A(a) + x_b\nu_A(b)\cdot = (\nu_A(a) + K_{ab}\nu_A(b))/(1 + K_{ab}) \qquad (3)$$

A similar equation is valid for X. In the special case where $\nu_A(a) = \nu_X(b)\cdot = \nu_{NH}$ and $\nu_A(b) = \nu_X(a)\cdot = \nu_N$, the combined line shape of A and X is depicted in Figure 2b. In the fast exchange region a line splitting arises given by[12−14]

$$\delta\nu = \Delta\nu(1 - K_{ab})/(1 + K_{ab}) \qquad \Delta\nu = \nu_N - \nu_{NH} \qquad (4)$$

If the low-temperature splitting $\Delta\nu$ is known, the equilibrium constant K_{ab} can be calculated from $\delta\nu$. In the symmetrical case where $K_{ab} = 1$, it follows that $\delta\nu = 0$, and only a single line is obtained in the fast exchange region of the degenerate exchange as depicted in Figure 2c.

The static disorder means that protons are localized but at two different centers; therefore, as a result of X-ray measurements, it is seen as delocalized between these two centers. The dynamic disorder means that the same X-ray picture is due to the exchange of the proton between these two positions. Unfortunately, the precision of X-ray measurements does not allow to obtain equilibrium constants of tautomeric processes by analysis of experimental effective bond lengths and thermal ellipsoids.

Experimental Section

Synthesis of *N,N*-Bisarylformamidines and Their ^{15}N-Labeled Analogs. *N,N*-Bisarylformamidines were obtained by the reaction of triethylorthoformate with the substituted anilines according to the know method of Claisen.[18]

$^{15}N,^{15}N$-Bisarylformamidines enriched to the 95% level were obtained using [^{15}N]aniline and the substituted (*p*-Br, *p*-NO_2) [^{15}N]anilines, and crystallization from n-heptane. The substituted [^{15}N]anilines were prepared from the respective [^{15}N]benzamides by the Hoffmann rearrangement.[19,20] The *p*-substituted [^{15}N]benzamides were synthesized from $^{15}NH_4Cl$ and the appropriate benzoyl chloride according to the method of Axenrod.[21] The crystals for XRD analysis were grown from anhydrous tetrahydrofuran or ethanolic solutions.

^{15}N CPMAS NMR Measurements. The ^{15}N CPMAS NMR spectra were recorded at 9.12 MHz using a Bruker NMR spectrometer CXP 100 equipped with a cryomagnet. For the measurements, a standard 7 mm DOTY CP MAS probe was used. Spinning speeds were between 2 and 2.5 kHz and large enough to obtain spectra where rotational side bands are smaller than the signal-to-noise ratio. The CP times were about 1.5 ms, and the repetition times were between 1 and 3 s. Between 500 and 2500 scans were accumulated for each spectrum. Chemical shifts were referenced to external solid $^{15}NH_4Cl$ located at −338.1 ppm from nitromethane.[22]

X-ray Diffraction Experiments. The X-ray measurements were made using a KM-4 diffractometer, with graphite-monochromated Cu Kα radiation. The data were collected at room temperature using the $\omega-2\theta$ scan techniques. The intensity of control reflections for the five compounds varied by less than 5%, and a linear correction factor was applied to account for this effect. The data were also corrected for Lorentz and polarization effects, but for four compounds no absorption correction was applied and only for *m*-Br were the data corrected for absorption.[23] These structures were solved by direct methods[24] and refined using SHELXL.[25] Refinement was based on F^2 for all reflections, except for those with very negative F^2. The weighted

(18) Claisen, L. *Liebigs Ann*. **1895**, *287*, 366.
(19) Lambert, J. B.; Stec, D., III *Org. Magn. Reson*. **1984**, *22*, 301.
(20) Ott, D. G. *Synthesis with stable isotopes of C, N, and O*; Wiley: New York, 1981.
(21) Axenrod, T.; Pregosin, P. S.; Wieder, M. J.; Becker, E. D.; Bradley, R. B.; Milne, G. W. A. *J. Am. Chem. Soc*. **1971**, *93*, 6536.
(22) Aguilar-Parrilla, F.; Männle, F.; Limbach, H.-H.; Elguero, J.; Jagerovic, N. *Magn. Reson. Chem*. **1994**, *32*, 699.
(23) Walker, J.; Stuart, J. *Acta Crystallogr*. **1983**, *A39*, 158.
(24) Sheldrick, G. M. *Acta Crystallogr*. **1990**, *A46*, 467.
(25) Sheldrick, G. M. *SHELXL93. Program for Refinement of Crystal Structure*; University of Göttingen: Germany, 1993.

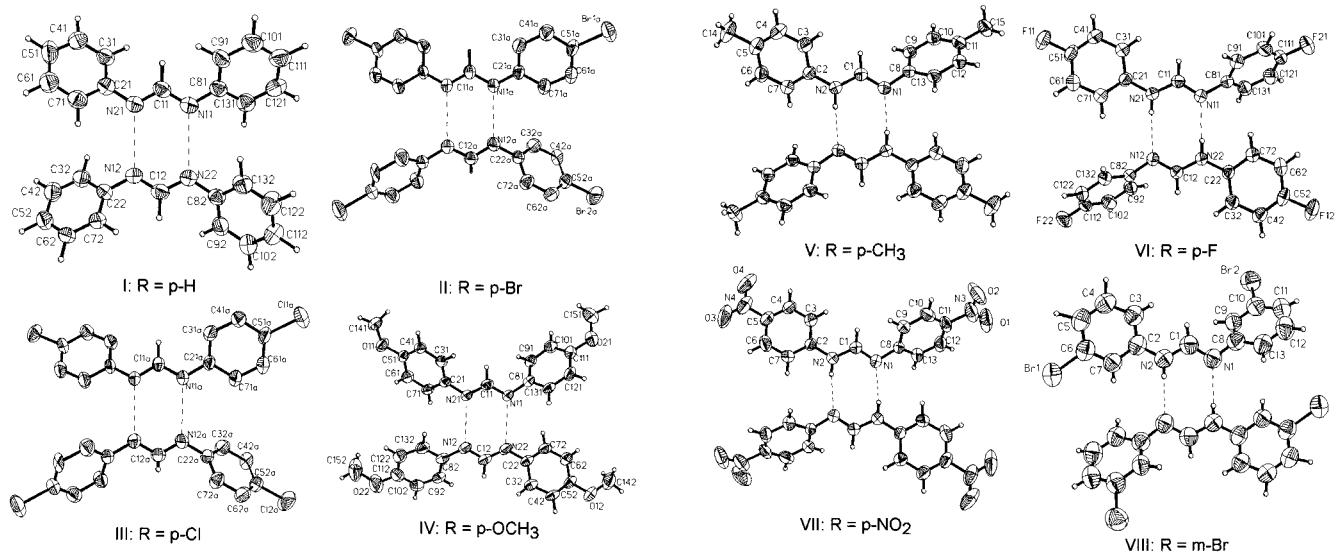

Figure 3. Crystal structures of bisarylformamidine dimers. The structures of **I**−**III** were adapted from refs 7−9.

R-factors (w*R*) and all goodness-of-fit (*S*) values are based on F^2. Conventional *R*-factors are based on *F* with *F* set to 0 for negative F^2. The observed criterion of $F^2 > 2\sigma(F^2)$ is used only for calculating *R*-factors and is not relevant to the choice of reflections for refinement. The *R*-factors based on F^2 are statistically about twice as large as those based on *F*, and the *R*-factors based on all data are even larger. Non-hydrogen atoms were refined anisotropically, whereas H-atoms were placed in calculated positions and their thermal parameters were refined isotropically. The H atoms connected with the amidine skeletons were located from difference map and refined isotropically. Atomic scattering factors were taken from ref 26.

Results

Some selected results of the X-ray measurements, structural computation, and crystal data for the *N*,*N*′-bis(*p*-X-phenyl)-formamidines **IV**−**VIII** are assembled in Table 1 and depicted in Figure 3 together with those of **I**−**III** studied previously.

The amidines studied were divided in three types, based on the value of the equilibrium constant K_{ab} of tautomerism measured by ^{15}N CPMAS NMR as described below. Type A refers to the case where the equilibrium constants of proton tautomerism K_{ab} are so small they cannot be determined by ^{15}N CPMAS NMR. In XRD, this case refers to "complete proton order", as depicted schematically in Figure 4a. Type B corresponds to degenerate case where $K_{ab} = 1$ within the margin of error of NMR, commonly referred to in XRD as the case of "dynamic disorder", as depicted schematically in Figure 4b. Type C corresponds to an intermediate case where $K_{ab} < 1$ which one could call "dynamic partial order". In principle, this classification is arbitrary and types A and B are only a subgroup of type C dimers.

N,*N*-Bisarylamidines of Type A. The ^{15}N CPMAS NMR spectra of type A amidines exhibit two position independent lines in the whole temperature range, split by $\delta\nu \approx \Delta\nu = \nu_N - \nu_{NH}$. A typical spectral set is shown in Figure 5 for the case of *N*,*N*′-bis(*p*-methyl)formamidine (**V**). The high-field line arises from the protonated nitrogen atoms, the low-field line arises from the nonprotonated ones, and the difference $\delta\nu = 110$ ppm. The line splitting is independent of temperature as expected according to eq 4 for an equilibrium constant of proton transfer which is zero within the margin of error in temperature range

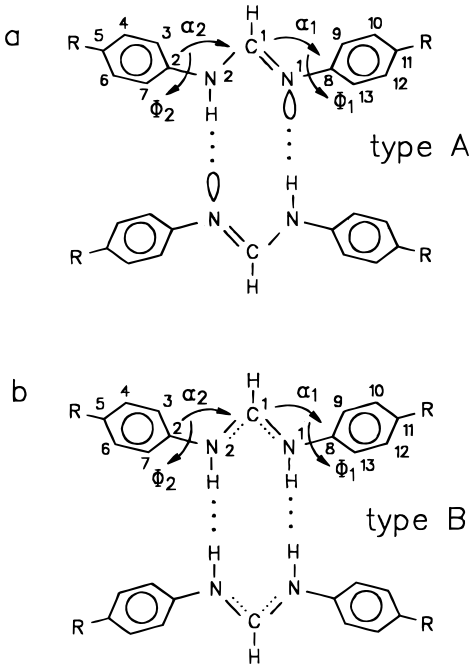

Figure 4. Simplified atom and bond angle number in cyclic *N*,*N*-bisarylformamidine dimers of types A and B.

covered. In other words, only one tautomer (a) can be observed, which we label as a. Nevertheless, if there is a small amount of b, it could interconvert slowly or rapidly to a. Within the margin of error, the two molecules in the dimer are equivalent, because otherwise one should observe four lines. The origin of the small shoulder of the high-field line could not be evaluated in this study.

As can be inferred from Figure 3, type A amidines such as **V** (*p*-CH_3), **VII** (*p*-NO_2), and **VIII** (*m*-Br) are centrosymmetric crystallographically; whereas, the dimer of **VI** (*p*-F) exhibits a slight deformation from the local centrosymmetry. In other words, in **VI** there are two independent molecules in the dimer differing only slightly one from another, with the bond lengths C1···N2 of 1.349 and 1.342 Å and C1···N1 bond lengths of 1.281 and 1.283 Å (Table 1).

***N*,*N*-Bisarylamidines of Type B.** The ^{15}N CPMAS NMR spectra of **II** (*p*-Br) have been described recently.[16] This molecule exhibits two lines for the amino and the imino nitrogen atoms only at low temperatures, as depicted in Figure 6. As

(26) *International Tables for X-ray Crystallography;* Kynoch Press (present Distributor Kluver Academic Publishers, Dordrecht): Birmingham, U.K., 1974; Vol. IV.

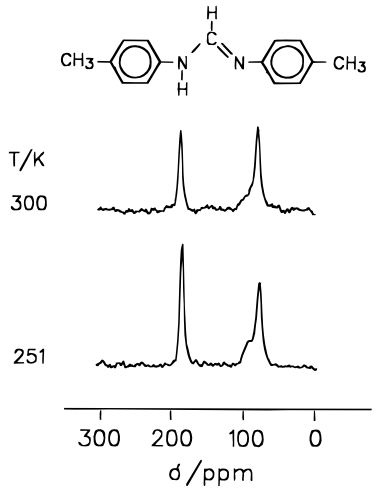

Figure 5. ^{15}N CPMAS NMR spectra of (**V**, type A) at different temperatures.

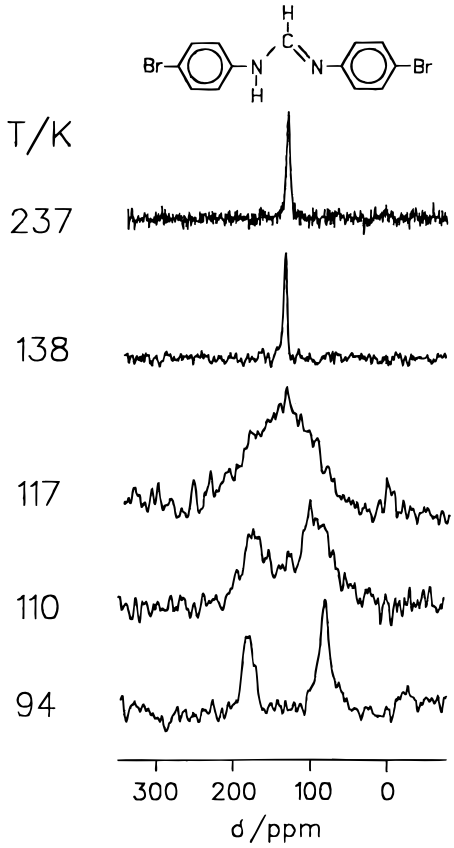

Figure 6. ^{15}N CPMAS NMR spectra of **II** (type B) at different temperatures.

temperature is increased, the lines broaden and coalesce into a single line, as predicted in Figure 2c for the case when $K_{ab} = 1$. Therefore, this molecule belongs to the type B. The rate constants determined by line shape analysis and ^{15}N T_1 relaxation analysis, showed that the proton transfer is in the nanosecond time scale at room temperature. Since small deviations from the value $K_{ab} = 1$ cannot be easily verified by NMR and since these measurements were only carried out down to 90 K, one could perhaps speculate that an asymmetric structure with $K_{ab} \ll 1$ could be realized at cryogenic temperatures. The crystallographic structure of this molecule shown in Figure 3 corresponds to the effective structure depicted schematically in Figure 4. In two cases (i.e., **II** and **III** (Figure 3)) a C_2 axis intersects the formyl carbon (C1) atoms.

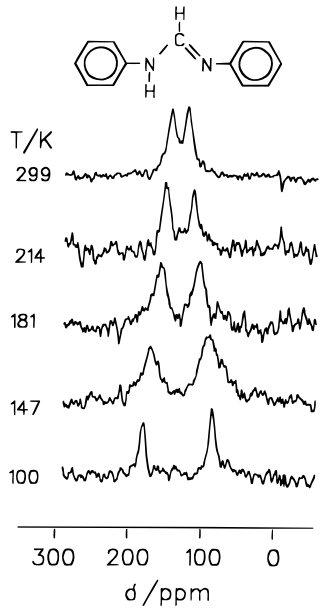

Figure 7. ^{15}N CPMAS NMR spectra of **I** at different temperatures.

A similar structure is also obtained for **III**, which was, therefore, classified as type B, although no NMR experiments were performed on this molecules.

The symmetry of **II** and **III** automatically resulted from the previous assumption of a *C*2/*c* space group.[8,9] However, we note that the XRD symmetries at room temperature are not perfect, and it is conceivable that XRD measurements at cryogenic temperatures may reveal a lower symmetry, i.e., space group *Cc*, corresponding to type A dimers. In order to determine whether the symmetry of Figure 3a is intrinsic or only realized within the margin of the experimental error, a Hamilton test[28] was performed on the XRD data, but it was not possible to differentiate between these two cases since the number of reflexes was not sufficient.

***N,N*-Bisarylamidines of Type C.** Amidine dimers of type C such as **I** and **IV** represent intermediate cases (i.e., type C) as illustrated for **I** in Figure 7 showing the variable-temperature ^{15}N CPMAS NMR spectra which are of the type of Figure 2b. With line shape analysis, rate and equilibrium constants can be obtained. At 100 K the process is in the second time scale, leading to two lines for the nonprotonated and protonated nitrogen atoms, separated by $\Delta\nu = 110$ ppm. At room temperature the proton transfer is fast, (i.e., in the milli- to microsecond time scale and a reduced splitting is observed, $\delta\nu = 20$ ppm from which an equilibrium constant of $K_{ab} = 0.8$ at room temperature can be calculated using eq 5.

The crystal structures of **I** and **IV** are included in Figure 3. Again, cyclic dimers are observed formed by two independent molecules, exhibiting substantial equalization of the C···N bond lengths. This is in line with the results of the refinement process. In this case both hydrogens are disordered with the site occupation factors equal to 0.5 and 0.5 for one hydrogen and partially disordered in the second hydrogen bond, with site occupation factors of 0.6 and 0.4. We are convinced that a similar situation is realized also in the case of compound **I**. Unfortunately, as the structure of this molecule was solved a

(27) Pauling, L. *The Nature of the Chemical Bond;* Cornell University Press: Cornell, NY, 1960, p 261.

(28) Hamilton, W. C. *International Tables for X-ray Crystallography;* Kynoch Press (present Distributor Kluver Academic Publishers, Dordrecht): Birmingham, U.K., 1974; Vol. IV, p 288.

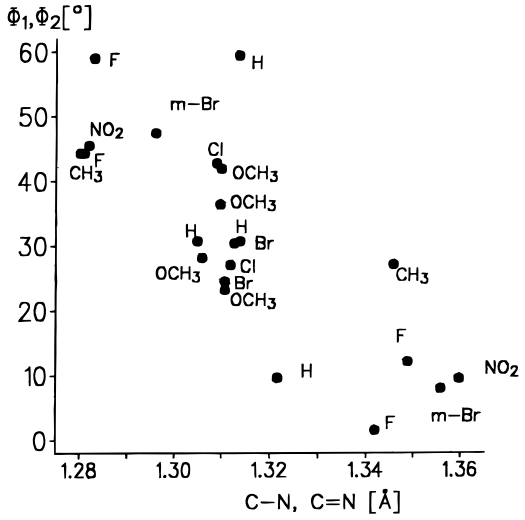

Figure 8. Relationship between twist angles ϕ of aromatic rings and carbon−nitrogen bond lengths (see Figure 4).

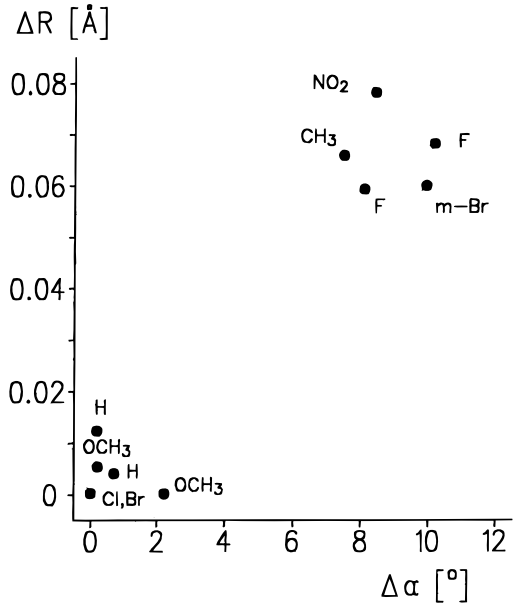

Figure 9. Relationship between ΔR = C1···N2−C1···N1 and $\Delta\alpha = \alpha_2 - \alpha_1$ (see Figure 4).

long time ago we were not able to recover the experimental data in order to repeat an alternative refinement of the hydrogen disorder.

Discussion

We have presented crystal structures and variable-temperature ^{15}N CPMAS NMR spectra of a number of *N,N′*-bisarylformamidines. All compounds crystallize as cyclic hydrogen-bonded dimers in *s-trans* configuration, according to Figure 1, and can in principle adopt two tautomeric states (a and b) interconverting by fast double proton transfers. Generally, the gas-phase degeneracy of this process is lifted in the crystalline state because of an interplay between the crystal packing forces and a reduction of the molecular symmetry. Depending on the amount of the reduction, the different amidines exhibit different equilibrium constants K_{ab} of the tautomerism. Examples were given for $K_{ab} \ll 1$ (type A), $K_{ab} = 1$ (type B), and the intermediate case (type C). Thus, a comparison of the structures of the different types can provide information about the question of which structural elements are related to hydrogen bonding and proton tautomerism of bisarylformamidines as discussed in the following.

Aryl Conformation and Proton Tautomerism. The following structural elements come into sight (i.e., the structures of the two amidine units, the conformations of the four aryl groups, and the relative orientation of two amidine units in a given dimer). The amidine units are essentially planar and can be characterized by the distances N1···C1 and C1···N2, their difference ΔR, and the valence angle N1−C1−N2 (see Figure 4). For type A amidines, nonzero values of ΔR are observed (Table 1) indicating distinct double-bond and single-bond character of CN in a given amidine unit, where the nitrogen atom involved in the single bond is protonated. In type B amidines, the dynamic proton disorder is then associated with a dynamic disorder of the nitrogen atoms which is, however, not resolved by XRD. Therefore, the two bond lengths N1···C1 and C1···N2 are effectively equal (i.e., $\Delta R = 0$ (Table 1)).

The type A amidines further exhibit different torsional angles ϕ_1 and ϕ_2 and valence bond angles α_1 and α_2 of the aryl groups of a given amidine molecule as defined in Figure 4. As indicated in Table 1, the torsional angles ϕ_2 of aryl groups attached to amino nitrogen atoms N_2 are smaller than the angles ϕ_1 of aryl groups attached to imino nitrogen atoms N1. Figure 8 shows a plot of the aryl twist-angle ϕ_1 as a function of the C1···N1 bond length and of ϕ_2 as a function of C1···N2· as a function of the carbon−nitrogen distance. In spite of a substantial scattering, an approximate linear decrease from about 60° to values close to 0 is observed. For each molecule of a dimer of type B, $\Delta\phi = \phi_1 - \phi_2 = 0$; however, the torsional angles can be different in both molecules (i.e., 27° and 30° in the case of **II** and 27° and 42.7° in the case of **III**). In the case of the valence angle differences $\Delta\alpha = \alpha_1 - \alpha_2$ we observe a correlation with ΔR as illustrated in Figure 9: for type A dimers both quantities are large, but zero for type B and small for type C dimers.

Finally, we observe that although each amidine unit is planar, the two amidine units of a dimer are not coplanar. However, the angle between the two planes is not related in any significant way to the equilibrium constant of tautomerism.

The observation of different conformations of the two aryl groups of a given amidine unit has some consequences for the double proton transfer in the dimers. Type A dimers exhibit only a crystallographic or local C_i symmetry (**V**−**VIII**) and are, therefore, characterized by an equilibrium constant $K_{ab} = k_{ab}/k_{ba} = x_b/x_a \ll 1$ of the double proton transfer. This effect is associated with a different conformation of the two aryl groups (i.e., valence bond and torsional angles) attached to the two nitrogen atoms of a given amidine unit. In this case, the forward rate constant k_{ab} is much smaller than the backward rate constant k_{ba}, but the absolute value of k_{ab} may be large. In order to produce a situation of a degenerate double proton transfer with $K_{ab} = 1$, the conformation of the two aryl groups of each amidine subunit must be the same. The latter is realized for amidine dimers of type B (**II** and **III**) which exhibit a crystallographic C_2 axis (i.e., the degeneracy of the proton tautomerism is understandable). Type C dimers exhibit an approximate local noncrystallographic C_2 (**I** and **IV**) and represent, therefore, an intermediate case where K_{ab} is found within the margin of error of NMR to be larger than zero but smaller than 1.

The degeneracy of the double proton transfer in type A amidines would be restored if the aryl groups could reorientate as indicated schematically in Figure 10a, but the crystal packing forces do not allow for this process to take place in the solid state. By contrast, in the liquid state, one can conceive a broad distribution of aryl conformations. In this case the double proton

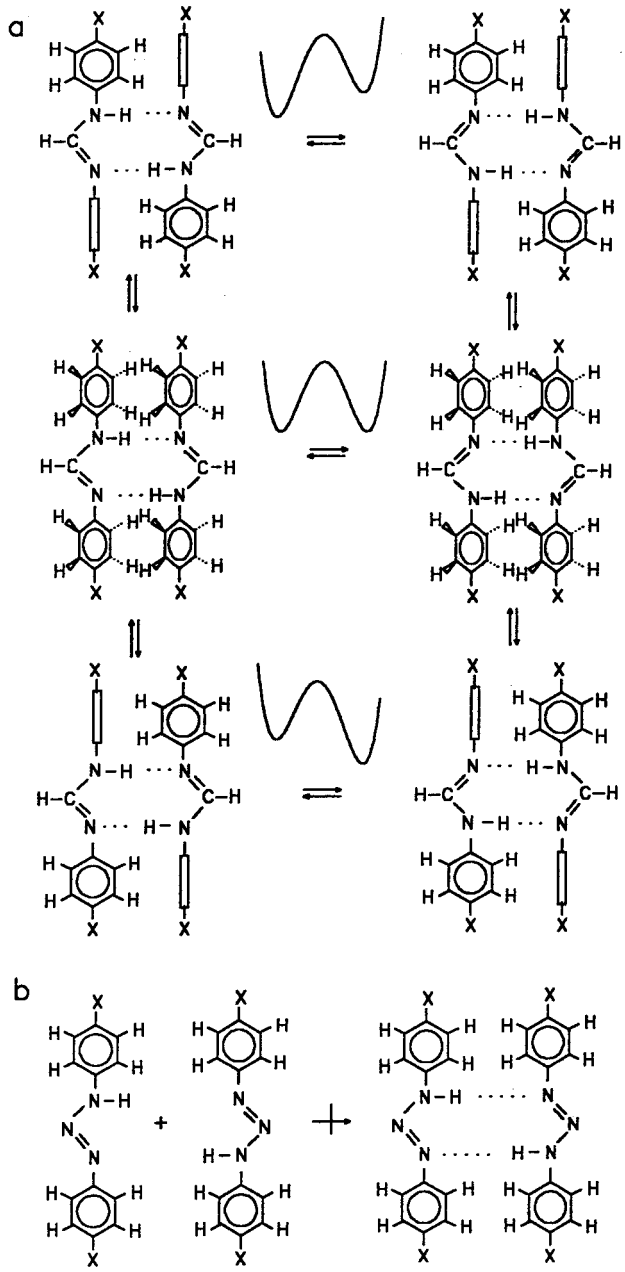

Figure 10. Aryl group torsion, double proton transfer, and hydrogen bonding in bisarylformamidines and bisaryltriazenes. One-dimensional schematic potential curves for the double proton transfer are included.

transfer can take place either along an asymmetric proton potential (Figure 1a, top and bottom) or along a symmetric potential (center). However, as the aryl reorientation can be fast in the liquid state the overall process is degenerate as long as the substitutents X in the aryl rings are the same.

Aryl Conformation and Hydrogen Bonding. The most obvious reason for the large aryl torsional angles in the amidine molecules is the steric interaction between the formyl proton H1 and aromatic protons H3 and H9. When the distance decreases, the torsional angle ϕ should increase; however, the balance can be somewhat restored by an valence angle α. Additionally, the other intermolecular interactions in the crystal lattice may also contribute to the variation of ϕ. Nevertheless, it seems that α is particularly large when ϕ is small (Table 1). This aryl group torsion is particularly important for the possibility of bisarylformamidines to form cyclic dimers. Thus, simple molecular models show that if the aryl groups were not twisted from the amidine plane, they would prevent another planar bisarylformamidine to approach and form a cyclic dimer. This phenomenon indeed occurs in the related bisaryltriazenes (Figure 10b). These molecules are planar and form chains in the solid state with angles of the order of 90° between each molecule.[29] Recently, it was shown that these molecules cannot form cyclic dimers in solution and are, therefore, not able to exchange their protons directly but only with the aid of a catalyst.[30] Thus, the aryl group conformation and as consequence the particular hydrogen-bond and proton transfer characteristics of bisarylformamidines are the consequence of a subtle interplay between intra- and intermolecular interactions. We note that the optimum approach is found in the type B dimers **II** and **III** which exhibit the shortest N···N distances in bisarylformamidine (i.e., 2.958 Å for **III** and 2.963 Å for **II**), whereas more than 3 Å is observed in the other amidines. Thus, aryl torsional angles of about 30° are the optimum values for the closest approach of two bisarylformamidines in a cyclic dimer.

Amidine Conformation and Electronic Properties. So far, we have not yet commented on the observation of why the valence and torsional angles are different for aryl groups attached to amino and imino nitrogen atoms of an amidine unit. The smaller torsional angle at the amino nitrogen can be rationalized with the higher π-electron density at the amino nitrogen and the increased coupling with the π-electron system of the adjacent aryl ring. A reduced electronic coupling between phenyl groups and the amidine unit at large twist angles has been reported for other *N*-phenylamidines.[5,6]

As mentioned above, a small torsional angle has the tendency to increase the valence angle in order to minimize the steric interaction between H1 and the aromatic H in *o*-position. On the other hand, this effect can also be understood in terms of the Bent−Walsh rule,[31] as discussed in the following. This rule states that the valence angle at an atom X in a π-electron system increases when the electronegativity of a substituent R attached to X is increased. For example, in the case of acid−base complexes R−O−H···B ↔ R−O$^-$···H−B$^+$ between pentachlorophenol and various bases, it has been observed that the valence angle at the *i*-carbon of R increases when the hydrogen-bond proton is shifted from the base toward the oxygen atom.[32] This effect has been interpreted in terms of the Bent−Walsh rule with an increasing electronegativity of the oxygen when the negative charge is removed. In the case of amidines, we compare the CNC valence angles, and the two substitutents are the lone pair in the nitrogen atoms differently bonded to the proton (i.e., N−H and N|···H. It is evident that the former exhibits a larger electronegativity than the latter, thus contributing to the larger valence angles at the amino nitrogen atoms.

Conclusions

A series of crystalline bisarylformamidines was studied by a combination of X-ray diffraction and ^{15}N solid state NMR which allowed us to elucidate a complicated interplay between molecular structure and hydrogen-bond dynamics in this type of compounds. Because of steric interactions, the aryl groups of bisarylformamidines cannot be coplanar with the amidine

(29) (a) Rumpel, H.; Limbach, H.-H.; Zachmann, G. *J. Phys. Chem.* **1989**, *93*, 1812. (b) Rumpel, H.; Limbach, H.-H. *J. Am. Chem. Soc.* **1989**, *111*, 5429.

(30) Männle, F.; Limbach, H.-H. *Angew. Chem.* **1996**, *108*, 477−479; *Angew. Chem., Int. Ed. Engl.* **1996**, *35*, 441.

(31) Bent, H. A. *Chem. Rev.* **1961**, *61*, 275.

(32) Wozniak, K.; Krygowski, T. M.; Kariuki, B.; Jones, W. *J. Mol. Struct.* **1991**, *248*, 331.

(33) Anulewicz, R., *Acta Crystallogr.* **1997**, *C53*, 345.

planes, as would be necessary for an optimized electronic coupling between the aryl and amidine π-systems. This is in contrast to the related bisaryltriazenes which are nearly planar.[33] However, in this case intermolecular steric interactions between the aryl groups prevent the formation of cyclic dimers formed by bisarylformamidines. In the latter, a thermally activated double proton transfer takes place which is degenerate only when the aryl group torsional and valence angles at both amidine nitrogen atoms are equal. Thus, the proton transfer and hydrogen bonding of bisarylformamidines are controlled by the amidine conformation which itself is the result of a subtle interplay between intra- and intermolecular forces.

Acknowledgment. Financial support from research grants of the Warsaw University (BW-1343/24/96) for R.A. and T.M.K. and the Deutsche Forschungsgemeinschaft, Bonn-Bad Godesberg, and the Fonds der Chemischen Industrie, Frankfurt, for H.-H.L. and F. M. are gratefully acknowledged.

Supporting Information Available: X-ray measurements, structural computation, and crystal data for the *N*,*N*′-bis(*p*-X-phenyl)formamidines **IV**−**VIII** (34 pages). See any current masthead page for ordering and Internet access instructions.

JA970699H